Eur. Phys. J. B (2015) 88: 191
DOI: 10.1140/epjb/e2015-50889-7

THE EUROPEAN PHYSICAL JOURNAL B

Regular Article

Enhancing and controlling single-atom high-harmonic generation spectra: a time-dependent density-functional scheme

Alberto Castro[1,2,a], Angel Rubio[3,4,5], and Eberhard K.U. Gross[6]

[1] ARAID Foundation, Edificio CEEI, María de Luna s/n, 50018 Zaragoza, Spain
[2] Institute for Biocomputation and Physics of Complex Systems (BIFI), and Zaragoza Center for Advanced Modelling (ZCAM), University of Zaragoza, 50018 Zaragoza, Spain
[3] Max Planck Institute for the Structure and Dynamics of Matter, Luruper Chaussee 149, 22761 Hamburg, Germany
[4] Center for Free-Electron Laser Science & Department of Physics, University of Hamburg, Luruper Chaussee 149, 22761 Hamburg, Germany
[5] Nano-Bio Spectroscopy Group and ETSF, Dpto. Fisica de Materiales, Universidad del País Vasco, CFM CSIC-UPV/EHU-MPC & DIPC, 20018 San Sebastián, Spain
[6] Max-Planck Institut für Mikrostrukturphysik, Weinberg 2, 06120 Halle, Germany

Received 30 December 2014 / Received in final form 1st April 2015
Published online 3 August 2015 –

Abstract. High harmonic generation (HHG) provides a flexible framework for the development of coherent light sources in the extreme-ultraviolet and soft X-ray regimes. However it suffers from low conversion efficiencies as the control of the HHG spectral and temporal characteristics requires manipulating electron trajectories on attosecond time scale. The phase matching mechanism has been employed to selectively enhance specific quantum paths leading to HHG. A few important fundamental questions remain open, among those how much of the enhancement can be achieved by the single-emitter and what is the role of correlations (or the electronic structure) in the selectivity and control of HHG generation. Here we address those questions by examining computationally the possibility of optimizing the HHG spectrum of isolated hydrogen and helium atoms by shaping the slowly varying envelope of a 800 nm, 200-cycles long laser pulse. The spectra are computed with a fully quantum mechanical description, by explicitly computing the time-dependent dipole moment of the systems using a time-dependent density-functional approach (or the single-electron Schrödinger equation for the case of H), on top of a one-dimensional model. The sought optimization corresponds to the selective enhancement of single harmonics, which we find to be significant. This selectivity is entirely due to the single atom response, and not to any propagation or phase-matching effect. Moreover, we see that the electronic correlation plays a role in the determining the degree of optimization that can be obtained.

1 Introduction

At sufficiently high intensities, matter no longer reacts linearly to light, and may re-emit at integer multiples (*harmonics*) of the frequency of the incoming source [1]. According to perturbation theory, the intensity of the harmonics decreases exponentially with their order. However, the spectrum of atoms and molecules exposed to very intense, typically infrared, laser pulses was found to present unexpectedly high harmonics [2,3], and its shape was observed to have a plateau extending non-perturbatively over many orders of magnitude – a process known as *high harmonic generation* (HHG) [4,5]. The light emitted in this manner is coherent and may reach the extreme ultraviolet and soft X-ray frequency regime. These properties can be of paramount importance for many technological and scientific purposes in ultrafast science – most notably, the generation of attosecond pulse trains or single isolated attosecond pulses, or the external seeding of free-electron lasers [6–8]. These advances open the path towards the coherent manipulation and control of matter at its natural time scale, since it becomes possible to follow the electron dynamics [9].

Unsurprisingly, a big effort has been devoted to first understanding the underlying physics, and then to controlling and fine-tuning the efficiency and spectral characteristics of the harmonic radiation. The latter can be done by modifying the non-linear medium, or by post-processing the signal with filters, gratings, etc. However, one advantageous alternative is to modify the characteristics of the parent pulse, which obviously will modify the spectral outcome. The most obvious manner of doing this is by systematically varying the defining parameters of this parent pulse [10–12]. However, the current availability of advanced pulse shaping tools [13], together with the development of closed-loop quantum control techniques [14],

[a] e-mail: acastro@bifi.es

provides a superior optimization alternative [15]. In this manner, the successful selective enhancement of harmonic orders could be achieved when using a hollow fiber container for the generating medium [16–18]. Gas jet (*free focusing*) geometries were also employed [19–21], but although some degree of control could be achieved (for example, the extension of the cut-off frequency), the very selective order enhancement or depletion obtained with the hollow fibers was not observed. This fact seems to imply that this type of selective enhancement cannot be explained from the single-atom response only; instead, the propagation effects present in the capillary set-up apparently play a fundamental role.

A full interpretation of the optimisation mechanisms can only be achieved with theoretical input, for which purpose one may utilise quantum simulations in combination with the theoretical branch of quantum optimal control [14,22] (QOCT). Recently, Schaefer and Kosloff [23,24] have addressed this task, showing the possibility of enhancing the emission at desired frequencies for simple few level systems and a 1D one electron system. Here we address, by simulations based on time-dependent density functional theory (TDDFT) [25,26] and 1D models of hydrogen and helium, the role of many electron interactions in the high harmonic generation, and provide compelling evidence that a single-atom HHG emission can be enhanced by few orders of magnitude in a controlled manner, with standard laser shaping techniques available in many experimental labs.

The *three-step* model successfully describes the key features of HHG [27–29], at least qualitatively. It combines a quantum description of the ionisation and recombination of the electrons, with a classical description of the intermediate electronic propagation. Lewenstein et al. [30] developed an approximate, mostly analytical, quantum description based on the *strong field approximation* (SFA): it neglects the contribution of excited bound states, the depletion of the ground state, and considers the continuum electrons to be free of the influence of the parent ion. This approach still makes use of the classical concept of "trajectory", which can be extracted from the phase of the wave function. A number of schemes for high-intensity laser-atom interaction develop on this concept of trajectory or "quantum orbit" [31]; some examples are the Volkov-eikonal approximation [32,33], the Coulomb-corrected SFA [34,35], the the Herman-Kluk propagator [36,37], or, very recently, Bohmian trajectories [38]. Finally, the most precise approach consists of propagating Schrödinger's equation [39–41], an expensive method that quickly becomes prohibitive as we increase the number of electrons. For one-electron problems the approach is perfectly feasible, and this fact has encouraged the use of the *single active electron* approximation (SAE), which assumes that only one electron is significantly disturbed by the field, and its evolution may be computed on the combination of the laser field and the potential originating by the parent ion.

This single electron picture is commonly used to describe recollision processes and HHG in atoms and relies on the fact that under HHG conditions there is one electron being emitted. However this does not imply the other electrons do not play a role. There is indeed no formal justification for the use of the SAE and in fact, many-body effects have been shown recently to play an important role in HHG providing an explanation of why heavier atoms emit stronger HHG than lighter ones [42] and the giant enhancement of He HHG at 100 eV [43]. However, the SAE has been successful in explaining a few features of the HHG spectra such as the spectral cutoff, the phase structure of the spectrum, and the generation of attosecond pulses.

In spite of all those experimental and theoretical efforts, it is clear that the topic of selective HHG generation deserves further microscopical analysis, and in this work, we explore the optimisation possibilities of one and two electron systems (the hydrogen and the helium atoms), isolating the single atom response, so that we can learn how much selectivity in the HHG spectrum can be obtained from isolated atoms. For this purpose, we employ a global optimisation scheme that acts on the envelope of the generating pulse, maintaining the fundamental frequency. For the case of helium, we report results obtained both with the single active electron approximation, and with TDDFT, in order to assess the influence of the electron-electron interaction in the optimisation process. As many-electron effects may be relevant, TDDFT appears as the ideal framework to capture them in the HHG spectra (see for example Ref. [44]) as it combines a very good compromise between accuracy and computational efficiency. The present optimisation scheme has been implemented in the first-principles code `octopus` [45,46], that allows the treatment of more complex molecular and extended systems. However for the purposes of the present work, it is better to stay at the simplest level of one and two electron systems. Larger electronic systems would offer a wider range of possibilities for HHG enhancement.

2 Theory

2.1 The HHG spectrum

Within the dipole approximation and in the length gauge, the experimentally measured harmonic spectrum can be theoretically approximated by the following formula (atomic units will be used hereafter):

$$H(\omega) = \left| \int_0^T dt \, \frac{\mathrm{d}^2}{dt^2} \left\langle \hat{\vec{\mu}} \right\rangle (t) e^{-\mathrm{i}\omega t} \right|^2 , \tag{1}$$

i.e. the power spectrum of the second derivative of the expectaction value of the dipole moment $\hat{\vec{\mu}} = -\sum_{i=1}^{N} \hat{\vec{r}}_i$ (see Ref. [47] for a discussion on the pertinence of using, alternatively, the first derivative or the dipole moment itself). This object is given by:

$$\frac{d^2}{dt^2} \left\langle \hat{\vec{\mu}} \right\rangle (t) = \left\langle \sum_{i=1}^{N} \nabla v(\hat{\vec{r}}_i) \right\rangle + N\varepsilon(t)\vec{\pi}, \tag{2}$$

where v is the (static) ionic potential, N is the number of electrons, $\varepsilon(t)$ is the laser pulse electric field amplitude, and $\vec{\pi}$ is the polarization vector. Note that this expression can be read as both the acceleration of the electronic system, and as the corresponding back-reaction of the nucleus (or nuclear center of mass, if we are dealing with a molecule). This is not surprising since the electromagnetic emission must be related with a charge acceleration. The expression corresponds, except for the mass factor, with the classical *force* acting on the nucleus, considered as a point particle. We will therefore rewrite equation (1) as:

$$H(\omega) = |\vec{f}(\omega)|^2, \tag{3}$$

where $\vec{f}(\omega)$ is the Fourier transform of:

$$\vec{f}(t) = \left\langle \sum_{i=1}^{N} \nabla v(\hat{\vec{r}}_i) \right\rangle + N\varepsilon(t)\vec{\pi}. \tag{4}$$

From a TDDFT perspective, the use of this force expression is convenient since it can be explicitly written as a density functional:

$$\vec{f}(t) = \int \mathrm{d}^3 r \; n(\vec{r},t)\nabla v(\vec{r}) + N\varepsilon(t)\vec{\pi}, \tag{5}$$

where $n(\vec{r},t)$ is the time-dependent electron density. This object can be obtained with TDDFT.

2.2 The density obtained from TDDFT calculations

The important point to notice is that the HHG spectrum may be explicitly computed solely in terms of this system electronic density. For systems with more than one electron, this fact is convenient since TDDFT allows to compute the density substituting the propagation of the real interacting system by the propagation of a system of fictitious non-interacting electrons, easier to handle: the "Kohn-Sham" (KS) system. It can be modeled with a set of single-particle orbitals forming the Slater determinant, whose equations of motion are usually called "time-dependent Kohn-Sham" (TDKS) equations:

$$\mathrm{i}\frac{\partial}{\partial t}\varphi_i(\vec{r},t) = -\frac{1}{2}\nabla^2\varphi_i(\vec{r},t) + v_{\mathrm{KS}}[n](\vec{r},t)\varphi_i(\vec{r},t), \tag{6}$$

$$\varphi_i(\vec{r},0) = \varphi_i^{\mathrm{gs}}(\vec{r}). \tag{7}$$

The initial values specified by equation (7) are given by the ground-state KS orbitals, computed with static DFT. The time-dependent density of the system may be retrieved from the KS orbitals with the simple formula:

$$n(\vec{r},t) = \sum_{i=1}^{N/2} \mu_i |\varphi_i(\vec{r},t)|^2, \tag{8}$$

where μ_i is the occupation of each orbital, which is equal to two if we consider a spin-compensated system of N electrons, doubly occupying a set of $N/2$ spatial orbitals φ_i $(i = 1, \ldots, N/2)$.

The potential that appears in those equations, v_{KS} (the "Kohn-Sham (KS) potential") is a functional of this density, and is defined as:

$$v_{\mathrm{KS}}[n](\vec{r},t) = v(\vec{r}) + \varepsilon(t)\vec{\pi}\cdot\vec{r} + v_{\mathrm{H}}[n](\vec{r},t) + v_{\mathrm{xc}}[n](\vec{r},t), \tag{9}$$

where the Hartree potential v_{H} is given by:

$$v_{\mathrm{H}}[n](\vec{r},t) = \int d^3r' \; \frac{n(\vec{r}',t)}{|\vec{r}'-\vec{r}|}, \tag{10}$$

and $v(\vec{r})$ is the static external potential. The time-dependent external potential for these one-electron equations is given by $\varepsilon(t)\vec{\pi}\cdot\vec{r}$.

Regarding the last term in the definition of the KS potential (Eq. (9)), the so-called "exchange and correlation potential": hereafter, we will restrict the discussion to one and two-electron systems, the extension to systems with larger number of electrons is straightforward in the TDDFT framework. The one-electron case obviously does not need a TDDFT treatment, although it may be treated as such by considering one single occupied orbital. For such one-orbital problem, the exchange and correlation potential must cancel the Hartree term:

$$v_{\mathrm{xc}}[n](\vec{r},t) = -v_{\mathrm{H}}[n](\vec{r},t), \tag{11}$$

so that the resulting equation reduces to the initial Schrödinger equation. For two-electron systems, we use the exact-exchange approximation (EXX) to the xc term, which for this two-electron case amounts to setting:

$$v_{\mathrm{xc}}[n](\vec{r},t) = -\frac{1}{2}v_{\mathrm{H}}[n](\vec{r},t). \tag{12}$$

Note that in this form TDDFT is identical to time-dependent Hartree-Fock that provides a good description of the non-linear properties of two-electron systems except for the description of charge-transfer excitations (see for example Ref. [48]). In any case, since we assume a spin-singlet configuration, only one orbital is necessary in the two electron case, too.

We have studied the two simplest atoms, hydrogen and helium. For the helium atom, we have used TDDFT with the exact-exchange functional (EXX). In order to assess the possible relevance of the electron-electron interaction, we have repeated the helium atom calculations employing the single active electron (SAE) approximation, which in this case amounts to freezing the Hartree, exchange and correlation functional to its ground-state value during the propagations. In this manner, we are effectively ignoring the electron-electron interaction during the propagation, and may gauge the relevance that it may have on the possibility of changing HHG spectra via smooth variations of the envelope function.

For the purpose of studying the HHG of atoms in linearly polarized pulses, one-dimensional (1D) models have been routinely employed in the past, and we have adhered to this practice, since it provides a good qualitative picture, while substantially reduces the computational cost.

The nucleus-electron interaction has the soft-Coulomb form:

$$v(x) = -\frac{Z}{\sqrt{a^2 + (x - x_0)^2}}, \tag{13}$$

for an electron placed at x and a nucleus of charge Z placed at x_0. The constant a may be tuned to reproduce some atomic property (e.g. ionization potential), although in this case we have simply fixed it to one for both hydrogen and helium. Likewise, the Hartree term given in equation (10) has to be *softened* in 1D, in our case using the same value for a:

$$v_{\mathrm{H}}[n](x,t) = \int dx' \, \frac{n(x',t)}{\sqrt{a^2 + (x' - x)^2}}. \tag{14}$$

The use of 1D representationss and modified interactions necessarily implies a loss of quantitative agreement with respect to the exact models. For example, the ionization potentials of helium and hydrogen are 0.90 and 0.50, respectively, whereas the ones that we get with this model are 0.75 and 0.67. These values could be matched by adjusting the softening parameter a; however we have preferred to set it to a common value.

Everything has been implemented in the `octopus` code [45,46]. The wavefunctions, potential, densities, etc. are represented in this code by the values they take at points of a real space grid. The Laplacian operator, needed to compute the kinetic part of the Hamiltonian, is computed using a 9-point finite difference formula. The propagations are performed by dividing the full time interval into short time steps $[t_0, t_1 = t_0 + \Delta t, t_2 = t_0 + 2\Delta t, \ldots, T]$, and approximating the short-time evolution operator $\hat{U}(t_{i+1}, t_i)$ with the exponential mid-point rule:

$$\hat{U}(t_{i+1}, t_i) \approx \exp\left\{-i\Delta t \hat{H}\left(t_i + \frac{1}{2}\Delta t\right)\right\}. \tag{15}$$

The action of the exponential on a state vector is computed by making use of the Lanczos polynomial expansion (see Ref. [49] for a discussion of the propagation schemes used in `octopus`). The full details about the combination of TDDFT and QOCT were explained in references [50,51].

2.3 The optimization

Usually, the electric field $\varepsilon(t)$ is factorised into a sinusoidal function determining the fundamental frequency ω_0, and an *envelope* function f that determines the overall laser-pulse shape:

$$\varepsilon(t) = f(t)\sin(\omega_0 t). \tag{16}$$

This factorisation – and the concept of a *fundamental frequency* – is meaningful for long and quasi-monochromatic pulses, but as the technology has reached the optical period limit, it has started to lose its relevance. Nevertheless, the existence of a fundamental frequency is implicit when speaking of harmonics, which are defined as radiation at integer multiples of precisely that frequency. These will only be well defined if the envelope function is *smooth* compared to the sinusoidal term, i.e. its frequencies are much lower than ω_0.

Therefore, in this work, we investigate the possibility of manipulating the envelope function f, leaving the sinusoidal factor $\sin(\omega_0 t)$ unchanged, in order to influence the shape of the HHG spectrum. This manipulation cannot be unconstrained, as the envelope must be composed of frequencies much lower than ω_0. Moreover, we have searched for solutions that preserve the fluence or total integrated energy of the pulse:

$$\overline{I} = \int dt \, \varepsilon^2(t). \tag{17}$$

This type of requirement of a specific structure for the solution field (in terms of frequencies, fluence, etc.) can be respected following essentially two routes: by imposing penalties on undesired features of the pulses in the definition of the optimising function, or by constraining from the beginning the search space. This latter option can be achieved by establishing a parametrisation of the control field (in this case, the envelope) that enforces the required condition, and is the route that we have chosen for this work. The search for the optimum is in this manner performed in the space of parameters that determine the control field; the remaining necessary ingredient is the definition of a *merit* function that encodes the physical requirements. Moreover, the assumption of low frequencies for f implies that the spectrum of ε is concentrated around ω_0. Therefore, the $N\varepsilon(t)\vec{\pi}$ term in equations (2), (4), and (5) does not contribute to the HHG spectrum in the region we are interested in and in the following we will safely ignore it.

The electric field amplitude will be determined by the specification of a set of M parameters $u_1, \ldots, u_M \equiv u$: $\varepsilon(t) = \varepsilon[u](t)$. The evolution of the TDKS system is in consequence also governed by the choice of parameters u, i.e. the orbitals and density are functionals of the parameters: $u \to \varphi[u]$, $u \to n[u]$. We may then use the tools of QOCT to find the set u that maximizes a given target function G, defined in terms of a functional of the density of the system, i.e.:

$$G[u] = \tilde{F}[n[u]]. \tag{18}$$

This functional $\tilde{F}$ is designed to favour the desired behaviour of the system (in this case, a certain form of the HHG spectrum, to be detailed below). Note that it is defined in terms of the system density, and not in terms of the full many-body wave function. This definition ensures that the substitution of the real by the KS system in the optimization entails no further approximation. The theory must however be developed in terms of a functional of the KS orbitals, which can be easily defined as:

$$F[\varphi] = \tilde{F}\left[\mu\varphi^*\varphi\right], \tag{19}$$

where μ is the occupation of the orbital φ, i.e. one or two for one- or two-electron calculations, respectively – since

we consider only one or two electron systems, there is only one KS involved.

We must now choose a form for F in such a way that its maximization leads to the desired HHG optimization, namely the selective increase of one harmonic peak – that should leave the neighboring ones as low as possible. There is substantial liberty to design F, and it is not evident what functional form should lead to better results. One possible choice is:

$$F[\varphi] = \sum_k \alpha_k H[\varphi](k\omega_0), \tag{20}$$

where α_k takes a positive value for the harmonic to be enhanced, and negative values for the ones that we wish to reduce. However, this choice proved to be problematic, since the modulation of the source signal with the envelope function leads to displacements, sometimes substantial, of the harmonic peaks with respect to the precise integer multiples $k\omega_0$. A general definition that solves this problem (and that includes the previous one as a particular case), is:

$$F[\varphi] = \int d\omega \alpha(\omega) H[\varphi](\omega) = \int d\omega \alpha(\omega) |\vec{f}[\varphi](\omega)|^2, \tag{21}$$

where we have made explicit the fact that both H and $\vec{f}$, defined in equations (1) and (4) are functionals of the time-dependent evolution for the system. The function α permits to establish some finite window around each harmonic peak $k\omega_0$, that will be positive for the harmonic orders that we want to enhance, and negative for the ones that we want to reduce. Finally, a third option is to seek for the maximum of the spectrum in these frequency windows around the harmonic orders, i.e.:

$$F[\varphi] = \sum_k \alpha_k \max_{\omega \in [k\omega_0 - \beta, k\omega_0 + \beta]} \{\log_{10} H[\varphi](\omega)\}, \tag{22}$$

where the real number β determines the size of the window.

Once the function G has been defined (through the definition of the target functional F), it remains to use some optimization algorithm to find the optimal u set. There are numerous options, and we may divide them on two groups, depending on whether or not they require the computation of the gradient of G – in addition of the computation of the function itself. The methods that employ the gradient are of course more efficient, as long as this gradient can itself be computed efficiently. The simplest scheme is steepest descents, but one can also use conjugate gradients or, in our case, the Broyden-Fletcher-Goldfarb-Shanno (GFBS) quasi-Newton method.

For the function G, the gradient is given by [50]:

$$\nabla G[u] = 2 \int_0^T dt \, \nabla \varepsilon[u](t) \mathrm{Im} \langle \chi[u](t) | \hat{\vec{r}} \cdot \hat{\pi} | \varphi[u](t) \rangle. \tag{23}$$

This expression uses an auxiliary orbital $\chi[u]$ defined by the following equations of motion:

$$\begin{aligned} \mathrm{i}\frac{\partial}{\partial t}\chi[u](\vec{r},t) = &-\frac{1}{2}\nabla^2 \chi[u](\vec{r},t) + v^*_{\mathrm{KS}}[n[u]](\vec{r},t)\chi[u](\vec{r},t) \\ &+ \hat{K}[\varphi[u](t)]\chi[u](\vec{r},t) \\ &- i\frac{\delta F[\varphi[u]]}{\delta \varphi^*[u](\vec{r},t)}, \end{aligned} \tag{24}$$

$$\chi[u](\vec{r},T) = 0. \tag{25}$$

The potential v_{KS} is the KS potential and the operator $\hat{K}[\varphi[u][t]]$ is defined as:

$$\begin{aligned} \hat{K}[\varphi[u](t)]\chi[u](\vec{r},t) = &-4\mathrm{i}\varphi[u](\vec{r},t) \\ &\times \mathrm{Im} \int \mathrm{d}^3 r' \, \chi^*[u](\vec{r}',t) f_{\mathrm{Hxc}}[n[u](t)](\vec{r},\vec{r}') \varphi[u](\vec{r}',t), \end{aligned} \tag{26}$$

where f_{Hxc} is the so-called *kernel* of the KS Hamiltonian, which, for our two-electron case treated within the EXX approximation, is given by: $f_{\mathrm{Hxc}}[n](\vec{r},\vec{r}') = \frac{1}{2}\frac{1}{|\vec{r}-\vec{r}'|}$, and is null for the one-electron case (zeroing the full $\hat{K}$ operator).

The functional derivative of F, needed in equation (24), for the HHG target defined in equation (21), is:

$$\frac{\delta F}{\delta \varphi^*(\vec{r},t)} = \vec{g}[\varphi](t) \cdot \nabla v(\vec{r}) \, \varphi(\vec{r},t), \tag{27}$$

where

$$\vec{g}[\varphi](t) = 2\mu \int d\omega \, \alpha(\omega) \mathrm{Re}\left[\vec{f}[\varphi](\omega) e^{-i\omega t}\right]. \tag{28}$$

However, we cannot compute this functional derivative for the target defined in equation (22) due to the presence of the "max" function, at least in a simple and efficient manner. In consequence, when using this target definition we could not make use of any of the optimization algorithms that make use of the gradient, and turned to the gradient-free NEWUOA algorithm [52], which is a very efficient scheme for optimization problems with a moderate number of degrees of freedom, such as the ones treated here.

In fact, for the optimizations attempted in this work, we observed numerically that the target of equation (22) provided much better results than the target of equation (21), and therefore we will only show below gradient-free optimizations; a recent publication [53], where the objective was the HHG cut-off extension, demonstrated gradient-based optimizations based on a target of the type given in equation (21).

Therefore, it remains to specify the set of parameters u that determine the envelope of the electric fields. The requirements are: (i) the envelope should have a given cut-off frequency; (ii) the field should smoothly approach zero at the end points of the propagation time interval; (iii) the total integral of the field should be zero, and (iv) the *fluence* or total integrated intensity of the pulse should have a

constant pre-defined value. This last condition is merely a choice, and not a physical constraint that experimentalists face.

The first step to parametrize the applied time-dependent electric field $\varepsilon(t)$ in order to enforce all these constraints is to expand the envelope in a Fourier series:

$$f(t) = \sum_{i=1}^{2L} f_i g_i(t), \tag{29}$$

where

$$g_i(t) = \begin{cases} \sqrt{\frac{2}{T}} \cos\left(\frac{2\pi}{T} i t\right) & (i = 1, \ldots, L) \\ \sqrt{\frac{2}{T}} \sin\left(\frac{2\pi}{T}(i-L)t\right) & (i = L+1, \ldots, 2L). \end{cases} \tag{30}$$

This series fixes the maximum possible (*cut-off*) frequency to $\frac{2\pi}{T}L$. Note that it explicitly omits the zero-frequency term, which is a desired restriction, in order to fulfill: $\int_0^T dt\ f(t) = 0$.

The manifold spanned by the f_i coefficients is not yet, however, our parameter space, since we still want to enforce the conditions $f(0) = f(T) = 0$, and fix the fluence: $\overline{I} = \int dt\ \varepsilon^2(t) = \overline{I}_0$. As discussed in reference [54], these conditions reduce the degrees of freedom from $2L$ to $2L-2$: the final parameters $u_1, \ldots u_{2L-2}$ are finally the hyperspherical angles that characterize a sphere of constant fluence, determining the Fourier coeffiencients: $f_i = f_i[u]$.

In all the OCT calculations to be shown below we have fixed the wavelength of the fundamental frequency ω_0 to 800 nm, a very common value used in laboratories equipped with a Ti:sapphire source. The total pulse duration is fixed to 200 cycles, $T = 200\ 2\pi/\omega_0$, which corresponds to 533 fs approximately. The envelope function $f(t)$ is then restricted to have frequencies no larger than $\omega_0/60$. The fluence (Eq. (17)) is then fixed to a value (around 5.0 a.u.) that ensures a sufficiently non-linear response of both the hydrogen and helium atoms, while not causing a substantial ionization. Fixing the fluence does not imply fixing the peak intensity; however the simultaneous existence of a maximum frequency puts a limit on it; in practice, the peak intensities observed in the optimal pulses are in the range of 5×10^{13}–10^{14} W/cm^2.

The optimization are started from randomly generated sets of parameters u. Since the procedure finds local maxima, we have performed several searches for each case, choosing afterwards the best among them. In order to have some "reference" to compare the optimal run to, we define a reference pulse as:

$$\varepsilon_{\mathrm{ref}}(t) = \varepsilon_0 \cos\left(\frac{\pi}{2}\frac{2t-T}{T}\right)\cos(\omega_0 t), \tag{31}$$

i.e. a cosinoidal envelope that peaks at $t = T/2$ with a value of ε_0, chosen to fulfill the fluence condition. The chosen peak amplitude ε_0 and frequency ω_0 imply a ponderomotive energy U_p of 0.069 a.u. This would in principle lead to expected cut-off harmonic frequencies ($3.17U_p + I_p$, where I_p is the ionization potential) of $16\omega_0$ and $17\omega_0$, respectively.

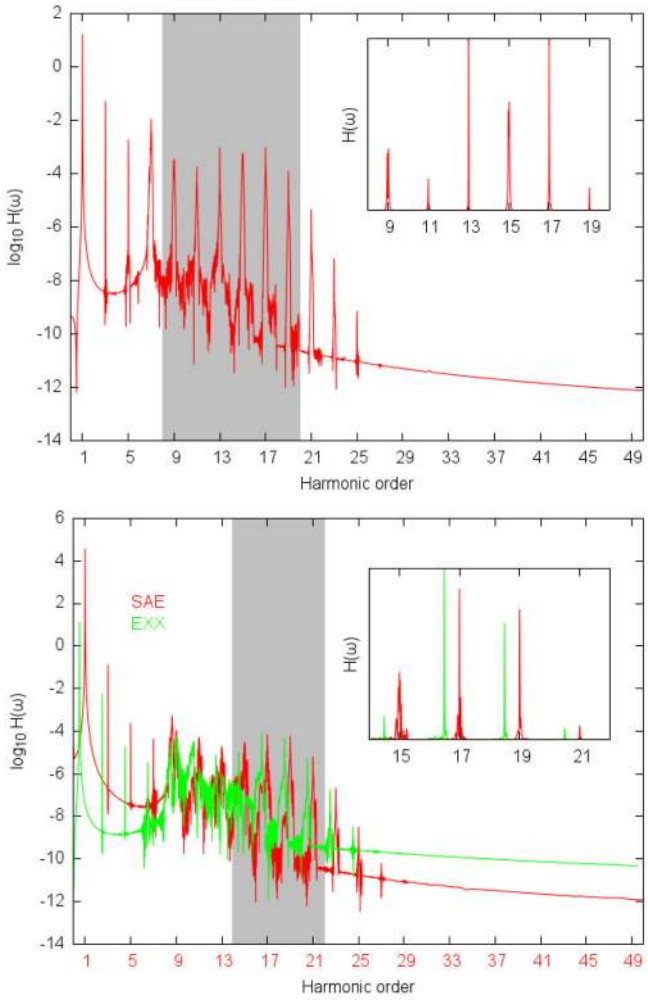

Fig. 1. HHG spectrum of the hydrogen (top) and He (bottom) atoms, with the reference pulse of equation (31). For the case of the He HHG spectra we show two results: one solving the TDDFT equations using the EXX functional (green) and the other solving the single-active-electron (SAE) (red) equation, commonly used by the strong-field community. To make more clear the comparison between EXX and SAE we shifted the SAE spectra by $0.5\omega_0$ in the x-axis. The shaded area contains the harmonics of interest. This area is also displayed in the inset, with a linear y-axis scale.

3 Results

The calculated HHG spectrum emitted by the hydrogen and helium atoms, irradiated by the reference pulse, is depicted in Figure 1. Note that the harmonic plateaus start their decline at the expected cut-off mentioned above. Also note that there is a range of harmonics with comparable intensities forming a plateau (9 to 19 in H and 15 to 21 in He). Because of this, we have selected that range (shaded in the plot) to perform the selective optimisations. The range is displayed, this time with a linear y-axis scale, in the inset. For the case of He we show the EXX and SAE results. As in He two electrons populate the only orbital in a spin-compensated configuration, the SAE approximation, in this case, consists in neglecting the interaction between

the electrons during the action of the field, freezing the potential to its ground state shape. In this adiabatic-DFT context, it amounts to ignoring the time-evolution of the Hartree, exchange and correlation potentials, and is useful to gauge the relevance that correlations may have on the HHG optimisation.

Let us discuss first the case of optimising the HHG spectra of H. We used the target given by equation (22) to optimise the odd orders from the 9th to 19th. To enhance the 9th harmonic, for example, we set $\alpha_9 = 5$, and $\alpha_{11} = \alpha_{13} = \alpha_{15} = \alpha_{17} = \alpha_{19} = -1$ (all other α_k are zero). In this manner, the sum of all coefficients is zero, avoiding any improvement of the merit function due to a mere overall reduction or increase of the spectrum. The results are displayed in Figure 2. From top to bottom, in the left panels, the spectra produced by the optimal fields for the 19th, 17th, ..., 9th harmonic. In the right panels, the optimal fields themselves; their envelopes in real time, as well as their power spectrum.

The resulting fields produce considerably higher harmonic outputs than the unshaped, reference field. To quantify this point we introduced an *enhancement factor* that is displayed in each plot, defined as:

$$\kappa_j = \frac{\max_{\omega\in[k\omega_0-\beta,k\omega_0+\beta]}\{H[\varphi](\omega)\}}{H_{\rm ref}(j\omega_0)}, \qquad (32)$$

where $H_{\rm ref}$ is the spectrum obtained with the reference field, and H the one obtained with the optimal field (the computation of the max function is not needed for the former, because due to the regularity of its envelope function, $H_{\rm ref}$ always peaks at the precise integer multiples $j\omega_0$). This enhancement factor greatly varies from case to case (i.e. it is 8 for $j = 13$, and 1006 for $j = 11$). Note that the plots do not share the same y-scale; they are scaled in each case to the value of the maximum of the plot.

We turn now our attention to the case of the helium atom, that contains two electrons. The interaction between these is treated here with TDDFT, within the EXX approximation. As in the previous case we performed optimisations based on the target given by equation (22), now for the orders 15th to 21st, fixing the coefficients α_k in an analogous manner. The results are displayed in Figure 3. From top to bottom, in the left panels, the spectra produced by the optimal fields for the 21st, 19th, 17th, and 15th harmonic. In the right panels, the optimal fields themselves.

The enhancement factors achieved are quite large, and as in the case of hydrogen, rather different from case to case. This rather large enhancement of the wanted harmonic is not accompanied by a full depletion of the neighbouring ones – in fact, they are also increased. This partial selectivity is also similar to the Hydrogen results. To quantify the role of electron-electron interactions we show in the same Figure 3 the SAE results (red curve). Qualitatively, the SAE results are not very different to the ones obtained with the EXX functional, in terms of intensity enhancements and selectivity. The fact that the calculated optimal fields and the spectra are different for both EXX and SAE illustrate not only the intrinsic non-linearity of

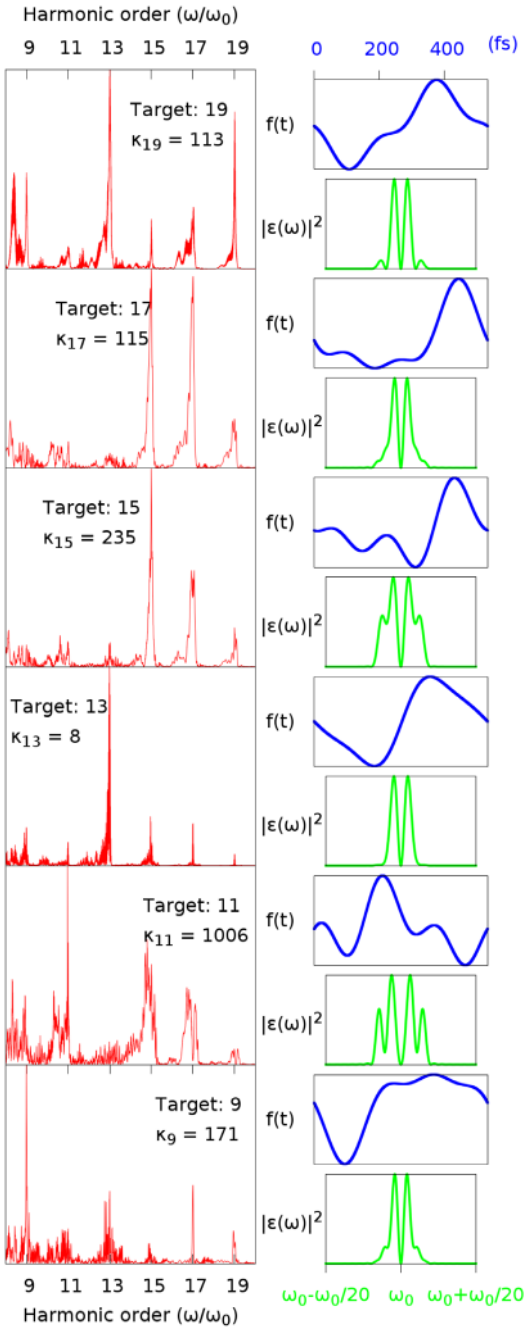

Fig. 2. Optimized HHG spectra (left panels), and corresponding optimal fields (right panels), for the hydrogen atom case. The optimal fields are plotted in the time domain (only the envelope function $f(t)$ is shown), and in the frequency domain. The HHG spectra are shown in a linear scale, normalized in each case up the value of the maximun value. The enhancement factor defined in equation (32) is also shown.

the optimisation algorithms and the rather large number of possible local maxima, but also the fact that electron interaction does play a role in the generation and optimisation of harmonics. Indeed, by looking in more detail to the results shown in Figure 3 for all cases except for the optimisation of the 17th harmonic, we see that SAE with respect to EXX provides a better selectivity and harmonic

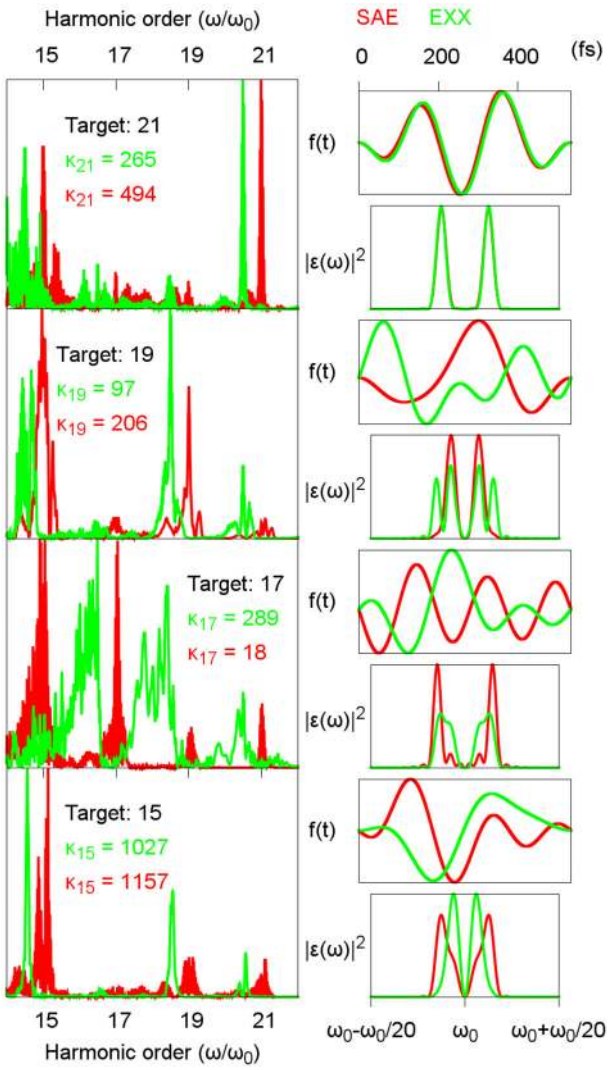

Fig. 3. Optimized HHG spectra (left panels), and corresponding optimal fields (right panels), for the helium atom case. As in Figure 1 we show in green the results within TDDFT using the EXX functional and in red the ones using the SAE approximation. The optimal fields are plotted in the time domain (only the envelope function $f(t)$ is shown), and in the frequency domain. The HHG spectra are shown in a linear scale, normalized in each case up the value of the maximun value. The enhancement factor defined in equation (32) is also shown. As in Figure 1, we shifted the SAE spectra by half a fundamental frequency in the x-axis.

enhancement, measured by the height of the desired harmonic and the quenching of the neighbouring ones. Therefore electron correlation seems to play a role in the optimisation of harmonics. This fact, together with the common knowledge that heavier noble gases emit stronger HHG radiation that light ones (whereas the SAE that predicts similar spectra) [55–57] support our findings about the limitations of the SAE approximation and the role of electron interactions. In fact we can expect larger enhancement factors to be reached by applying the present optimisation techniques to heavier atomic/molecular systems.

4 Conclusion

In conclusion, we have investigated, by theoretical means, the possibility of tuning the shape of the HHG spectrum of the hydrogen and helium atoms by shaping the slowly varying envelope of a 800 nm, 200-cycles long laser pulses. For this purpose, we have optimised a functional designed to enhance selected harmonics. The allowed modifications of the pulse are very constrained, since we enforce a maximum envelope frequency no larger than 1/60 of the fundamental frequency. This means very slowly varying envelopes. However, the picture that emerges of our analysis is that these relatively small modifications produce strong variations of the spectra, allowing for significative increases of the harmonic intensities. These enhancements are not fully selective, since the neighbouring harmonics also increase, but to a lesser extent. The outcome depends of the precise definition of the target functional, which is a topic to be investigated further. There is ample freedom to choose this object, and a different option may yield better selectivity – while perhaps reducing the total enhancement, or vice-versa.

The spectra have been computed with a fully quantum mechanical description, by explicitly computing the time-dependent dipole moment of the systems. The results presented here correspond to the single-atom response – we have not propagated Maxwell's equations in a atomic gaseous medium. Therefore, this work shows to which extent this single-atom response is significantly altered by the envelope of the laser pulse, even for the small modifications allowed in our scheme. We have shown that few orders of magnitude HHG enhancement factor can be reached at the single-atom level. Moreover, our results illustrate the role of electron-electron interactions in this optimisation and control of HHG.

This work was supported by the European Commission within the FP7 CRONOS project (Grant number 280879). A.R. acknowledges financial support from the European Research Council Advanced Grant DYNamo (ERC-2010- AdG-267374), Spanish Grant (FIS2013-46159-C3-1-P), Grupos Consolidados UPV/EHU del Gobierno Vasco (IT578-13), and COST Actions CM1204 (XLIC) and MP1306 (EUSpec). A.C. acknowledges support from the Spanish Grant FIS2013-46159-C2-2-P. All authors contributed equally to this article.

References

1. P.A. Franken, A.E. Hill, C.W. Peters, G. Weinreich, Phys. Rev. Lett. **7**, 118 (1961)
2. A. McPherson, G. Gibson, H. Jara, U. Johann, T.S. Luk, I.A. McIntyre, K. Boyer, C.K. Rhodes, J. Opt. Soc. Am. B **4**, 595 (1987)
3. M. Ferray, A.L. Huillier, X.F. Li, L.A. Lompré, G. Mainfray, C. Manus, J. Phys. B **21**, L31 (1988)
4. O. Smirnova, M. Ivanov, *Multielectron High Harmonic Generation: Simple Man on a Complex Plane* (Wiley-VCH Verlag GmbH and Co. KGaA, 2014), pp. 201–256

5. K.L. Ishikawa, in *Advances in Solid State Lasers Development and Applications*, edited by M. Grishin (Intech, 2010), Chap. 19, pp. 439–464
6. M. Hentschel, R. Kienberger, C. Spielmann, G.A. Reider, N. Milosevic, T. Brabec, P. Corkum, U. Heinzmann, M. Drescher, F. Krausz, Nature **414**, 509 (2001)
7. A. Wirth et al., Science **334**, 195 (2011)
8. T. Brabec, F. Krausz, Rev. Mod. Phys. **72**, 545 (2000)
9. M. Drescher, M. Hentschel, R. Kienberger, M. Uiberacker, V. Yakovlev, A. Scrinzi, T. Westerwalbesloh, U. Kleineberg, U. Heinzmann, F. Krausz, Nature **419**, 803 (2002)
10. D. Lee, J.H. Kim, K.H. Hong, C. Nam, Phys. Rev. Lett. **87**, 243902 (2001)
11. Z. Chang, A. Rundquist, H. Wang, M.M. Murnane, H.C. Kapteyn, Phys. Rev. Lett. **79**, 2967 (1997)
12. H.T. Kim, D.G. Lee, K.H. Hong, J.H. Kim, I.W. Choi, C.H. Nam, Phys. Rev. A **67**, 051801 (2003)
13. A.M. Weiner, Rev. Sci. Instrum. **71**, 1929 (2000)
14. C. Brif, R. Chakrabarti, H. Rabitz, New J. Phys. **12**, 075008 (2010)
15. C. Winterfeldt, C. Spielmann, G. Gerber, Rev. Mod. Phys. **80**, 117 (2008)
16. R. Bartels, S. Backus, E. Zeek, L. Misoguti, G. Vdovin, I.P. Christov, M.M. Murnane, H.C. Kapteyn, Nature **406**, 164 (2000)
17. R. Bartels, S. Backus, I. Christov, H. Kapteyn, M. Murnane, Chem. Phys. **267**, 277 (2001)
18. T. Pfeifer, D. Walter, C. Winterfeldt, C. Spielmann, G. Gerber, Appl. Phys. B **80**, 277 (2005)
19. D.H. Reitze et al., Opt. Lett. **29**, 86 (2004)
20. P. Villoresi, S. Bonora, M. Pascolini, L. Poletto, G. Tondello, C. Vozzi, M. Nisoli, G. Sansone, S. Stagira, S.D. Silvestri, Opt. Lett. **29**, 207 (2004)
21. D. Walter, Ph.D. thesis, University of Würzburg, 2006
22. J. Werschnik, E.K.U. Gross, J. Phys. B **40**, R175 (2007)
23. I. Schaefer, R. Kosloff, Phys. Rev. A **86**, 063417 (2012)
24. I. Schaefer, Master's thesis, Fritz Haber Center, Institute of Chemistry, The Hebrew University of Jerusalem, 2012
25. E. Runge, E. Gross, Phys. Rev. Lett. **52**, 997 (1984)
26. *Fundamentals of Time-Dependent Density Functional Theory*, Lecture Notes in Physics, edited by M.A.L. Marques, N.T. Maitra, F.M.S. Nogueira, E.K.U. Gross, A. Rubio (Springer, Berlin, Heidelberg, 2012), Vol. 837
27. J.L. Krause, K.J. Schafer, K.C. Kulander, Phys. Rev. Lett. **68**, 3535 (1992)
28. K.J. Schafer, B. Yang, L.F. DiMauro, K.C. Kulander, Phys. Rev. Lett. **70**, 1599 (1993)
29. P.B. Corkum, Phys. Rev. Lett. **71**, 1994 (1993)
30. M. Lewenstein, P. Balcou, M.Y. Ivanov, A. L'Huillier, P.B. Corkum, Phys. Rev. A **49**, 2117 (1994)
31. P. Saliéres et al., Science **292**, 902 (2001)
32. O. Smirnova, M. Spanner, M. Ivanov, Phys. Rev. A **77**, 033407 (2008)
33. O. Smirnova, M. Spanner, M. Ivanov, J. Phys. B **39**, S307 (2006)
34. S. Popruzhenko, D. Bauer, J. Mod. Opt. **55**, 2573 (2008)
35. T.M. Yan, S.V. Popruzhenko, M.J.J. Vrakking, D. Bauer, Phys. Rev. Lett. **105**, 253002 (2010)
36. M.F. Herman, E. Kluk, Chem. Phys. **91**, 27 (1984)
37. G. van de Sand, J.M. Rost, Phys. Rev. Lett. **83**, 524 (1999)
38. J. Wu, B.B. Augstein, C. Figueira de Morisson Faria, Phys. Rev. A **88**, 063416 (2013)
39. K. Kulander, K. Schafer, J. Krause, Laser Phys. **3**, 359 (1993)
40. X.M. Tong, S.I. Chu, Chem. Phys. **217**, 119 (1997)
41. A. Bandrauk, S. Chelkowski, D. Diestler, J. Manz, K.J. Yuan, Phys. Rev. A **79**, 023403 (2009)
42. A. Gordon, F.X. Kärtner, N. Rohringer, R. Santra, Phys. Rev. Lett. **96**, 223902 (2006)
43. S. Pabst, R. Santra, Phys. Rev. Lett. **111**, 233005 (2013)
44. C.A. Ullrich, S. Erhard, E.K.U. Gross, in *Super Intense Laser Atom Physics IV*, NATO ASI Series 3/13, edited by H.G. Muller, M.V. Fedorov (Kluwer, 1996), pp. 267−284
45. M.A.L. Marques, A. Castro, G.F. Bertsch, A. Rubio, Comput. Phys. Commun. **151**, 60 (2003)
46. A. Castro, H. Appel, M. Oliveira, C.A. Rozzi, X. Andrade, F. Lorenzen, M.A.L. Marques, E.K.U. Gross, A. Rubio, Phys. Stat. Sol. B **243**, 2465 (2006)
47. B. Sundaram, P.W. Milonni, Phys. Rev. A **41**, 6571 (1990)
48. J.I. Fuks, P. Elliott, A. Rubio, N.T. Maitra, J. Phys. Chem. Lett. **4**, 735 (2013)
49. A. Castro, M. Marques, A. Rubio, J. Chem. Phys. **121**, 3425 (2004)
50. A. Castro, J. Werschnik, E. Gross, Phys. Rev. Lett. **109**, 153603 (2012)
51. A. Castro, E. Gross, in *Fundamentals of Time-Dependent Density Functional Theory*, Lecture Notes in Physics, edited by M.A. Marques, N.T. Maitra, F.M. Nogueira, E. Gross, A. Rubio (Springer Berlin/Heidelberg, 2012), Vol. 837, pp. 265–276
52. M.J.D. Powell, IMA J. Numer. Anal. **28**, 649 (2008)
53. J. Solanpää, J.A. Budagosky, N.I. Shvetsov-Shilovski, A. Castro, A. Rubio, E. Räsänen, Phys. Rev. A **90**, 053402 (2014)
54. K. Krieger, A. Castro, E.K.U. Gross, Chem. Phys. **391**, 51 (2011)
55. C.G. Wahlström, J. Larsson, A. Persson, T. Starczewski, S. Svanberg, P. Salières, P. Balcou, A. L'Huillier, Phys. Rev. A **48**, 4709 (1993)
56. E. Constant, D. Garzella, P. Breger, E. Mével, C. Dorrer, C. Le Blanc, F. Salin, P. Agostini, Phys. Rev. Lett. **82**, 1668 (1999)
57. A. Gordon, F.X. Kärtner, N. Rohringer, R. Santra, Phys. Rev. Lett. **96**, 223902 (2006)